# What Determines the Wave Function of Electron-Hole Pairs in Polariton Condensates?

Kenji Kamide* and Tetsuo Ogawa

*Department of Physics, Osaka University, Toyonaka, Osaka 560-0043, Japan*

(Received 29 November 2009; revised manuscript received 1 July 2010; published 26 July 2010)

The ground state of a microcavity polariton Bose-Einstein condensate is determined by considering experimentally tunable parameters such as excitation density and detuning. During a change in the ground state of Bose-Einstein condensate from excitonic to photonic, which occurs as the excitation density is increased, the origin of the binding force of electron-hole pairs changes from Coulomb to photon-mediated interactions. The change in the origin gives rise to the strongly bound pairs with a small radius, like Frenkel excitons, in the photonic regime. The phase diagram obtained provides valuable information that can be used to build theoretical models for each regime.

DOI: 10.1103/PhysRevLett.105.056401 PACS numbers: 71.36.+c, 03.75.Hh, 71.35.Lk, 73.21.−b

Microcavity polaritons—photoexcited electrons and holes strongly coupled with photons in a microcavity—have been observed to exhibit Bose-Einstein condensation (BEC) [1,2]. Because of the light-matter coupling, the polariton has an extremely small mass about $10^{-4}$ times the free-electron mass; the small mass results in a high critical temperature and low critical density. BEC can be realized even at room temperature [3], which is remarkable considering that it had been difficult to realize BEC in exciton systems for a long time [4]. Microcavity polaritons are dissipative particles due to the short lifetime of photons and inelastic scattering of excitons. Therefore, the polariton BEC is in a nonequilibrium stationary state with a balance between pumping and losses [5,6]. However, the polariton BEC has many similarities with thermal equilibrium BEC [7]. It shows several evidences for the superfluidity: the Goldstone mode [8], the quantized vortices [9], and the Landau critical velocity [10].

Such a stationary state appears to be well described by the ground state of a closed microcavity polariton system, when the polariton lifetime is longer than the thermalization time [5,11]. In this Letter, assuming such a situation, we determine the ground state with a fixed excitation density at absolute zero as a function of experimentally variable parameters: excitation density, detuning [12], and ultraviolet cutoff determined by the lattice constant. In past studies, mean-field theories have been used to discuss the two limits—low excitation density [13,14] and high excitation density [15]—by considering two different models. These theories are complementary [16], but their relation is somewhat ambiguous. We investigate the intermediate density region as well, where the electron-hole ($e$-$h$) wave function of the relative motion becomes important. We show that the ground state energy and wave function gradually change from those of excitons to photons as the excitation density increases. It is also shown that the $e$-$h$ wave function narrows as the photonic fraction increases, which is accompanied by a change in the binding force from Coulombic force to photon-mediated force.

We consider polaritons in a two-dimensional (2D) quantum well embedded in a microcavity [1]. The polariton systems are described by the Hamiltonian $H = H_{\rm el} + H_{\rm el\text{-}el} + H_{\rm ph} + H_{\rm el\text{-}ph}$ [15] given by

$$H_{\rm el} = \sum_k \varepsilon_e(k) a_k^\dagger a_k + \varepsilon_h(k) b_k b_k^\dagger, \tag{1}$$

$$H_{\rm el\text{-}el} = \sum_q U_q {:}\rho_q \rho_{-q}{:}, \tag{2}$$

$$H_{\rm ph} = \sum_k \left(\sqrt{(ck)^2 + (\hbar\omega_c)^2} - \mu\right) \psi_k^\dagger \psi_k, \tag{3}$$

$$H_{\rm el\text{-}ph} = -g \sum_{k,q} (\psi_q a_{k+q}^\dagger b_k + \psi_q^\dagger b_{k+q}^\dagger a_k), \tag{4}$$

where $\varepsilon_{e,h}(k)$ $[= \hbar^2 k^2/2m_{e,h} + (E_g - \mu)/2]$ and $U_q$ $[=(\pi e^2/\epsilon^* Sq)]$ are the electronic dispersion in an effective mass approximation and the Coulomb interaction, respectively. Further, $a_k$, $b_k$, and $\psi_k$ are the annihilation operators of the conduction and valence electrons and photons with momentum $k$, respectively. Fourier transform of the density operator given by $\rho_q = \sum_k (a_{k+q}^\dagger a_k - b_{k-q} b_k^\dagger)$. The zero-point frequency of the cavity photons is $\omega_c$, and detuning is defined as $d = (\hbar\omega_c - E_g)/\varepsilon_0$, where $\varepsilon_0$ is the three-dimensional (3D) exciton Rydberg. The light-matter coupling constant is given by $g = d_{\rm cv}\sqrt{2\pi\hbar\omega_c/\epsilon^* S L_{\rm cav}}$, where $S$ and $L_{\rm cav}$ are the 2D area of the quantum well and the effective cavity length [17]. The momentum dependence of the dipole coupling is neglected here. Instead, a momentum cutoff $k_c$ is introduced so as to restrict the electronic states contributing to the polariton formation to $|k| < k_c$. It is smaller than or roughly equal to the inverse of lattice spacing (e.g., $60/a_0$ for a GaAs-based microcavity, with $a_0$ being the exciton Bohr radius). Considering the coherent state of polarizations and photons, the mean-field ground state of a polariton condensate is given by

 

$$|\Phi\rangle = e^{(\lambda\psi_0^\dagger - \lambda\psi_0)}\prod_k (e^{i\chi_k}u_k + v_k a_k^\dagger b_k)|\mathrm{vac}\rangle, \quad (5)$$

where $|\mathrm{vac}\rangle$ denotes the vacuum state with no conduction electrons, no valence holes, and no excited photons. Variational wave functions of this type have been used successfully in degenerate fermionic atoms with Feshbach resonance [18,19], being in a close analogy with the polaritons. Since we keep $u_k^2 + v_k^2 = 1$, the phase-space filling effect of fermions is automatically incorporated. The variational parameters $\lambda$, $\chi_k$, $u_k$, and $v_k$ are determined by the minimization of the total energy $E(= \langle H + \mu N_{\mathrm{ex}}\rangle)$ for fixed excitation number $N_{\mathrm{ex}}$, which is given by the expression $\sum_k \langle \psi_k^\dagger \psi_k + (a_k^\dagger a_k + b_k b_k^\dagger)/2\rangle$. In the coherent state, all the $e$-$h$ pairs are found to have the same phase: $\chi_k = 0$ [13]. After angular integration, the mean-field energy per excitation $\varepsilon$ $(= E/N_{\mathrm{ex}})$ and the total excitation density $\rho_{\mathrm{ex}}$ $(= N_{\mathrm{ex}}/S)$ are given by

$$\varepsilon/\varepsilon_0 = \frac{R_s^2}{a_0^2}\bigg(d\tilde{\lambda}^2 + \frac{1}{2}\int_0^{\kappa_c}\kappa^3 v_k^2 d\kappa - \tilde{g}\,\tilde{\lambda}\int_0^{\kappa_c}\kappa u_k v_k d\kappa - \int_0^{\kappa_c}\int_0^{\kappa_c} Q_{\kappa_1,\kappa_2}(v_{k1}^2 v_{k2}^2 + u_{k1}v_{k1}u_{k2}v_{k2})d\kappa_1 d\kappa_2\bigg), \quad (6)$$

$$\rho_{\mathrm{ex}} = \frac{1}{\pi a_0^2}\bigg(\tilde{\lambda}^2 + \frac{1}{2}\int_0^{\kappa_c}\kappa v_k^2 d\kappa\bigg) = \frac{1}{\pi R_s^2}, \quad (7)$$

where $\kappa = ka_0$, $\kappa_c = k_c a_0$, $Q_{\kappa_1,\kappa_2} = \frac{2\kappa_1\kappa_2}{\pi(\kappa_1+\kappa_2)}K_1(\frac{4\kappa_1\kappa_2}{(\kappa_1+\kappa_2)^2})$ with $K_1(z)$ being the complete elliptic integral of the first kind, $R_s$ is the mean separation, $\tilde{\lambda}$ $(= \lambda\sqrt{\pi a_0^2/S})$ is the normalized photon field, and $\tilde{g}$ $(= g\sqrt{S/\pi a_0^2 \varepsilon_0^2})$ is a dimensionless coupling constant. It is difficult to determine an infinite number of variational parameters; hence, we use an interpolating wave function for the excitonic constituent [20] in this 2D polariton case:

$$\frac{u_k v_k}{u_k^2 - v_k^2} = \frac{\zeta\,\mathrm{sgn}[(\kappa/2)^2 - X]}{\sqrt{1+(\kappa/2)^2}\sqrt{(\kappa/2)^4 - 2X(\kappa/2)^2 + \eta^2 X^2}}. \quad (8)$$

This form of the wave function is chosen so as to guarantee correct result for three limiting cases: (i) exciton BEC ($\tilde{\lambda}^2 \ll a_0^2/R_s^2$, $\zeta \ll 1$, $X = -1$, $\eta = 1$)—the low-density limit with negligible photonic fraction, (ii) $e$-$h$ BCS [$\tilde{\lambda}^2 \ll a_0^2/R_s^2$, $\zeta \ll 1$, $X = (k_F a_0/2)^2$, $\eta = 1$]—the high-density limit with negligible photonic fraction, (iii) photonic BEC ($\tilde{\lambda}^2 \to a_0^2/R_s^2$, $\eta = 0$, $\zeta/\sqrt{|X|}$ is finite while $\zeta = \infty$, $X = -\infty$)—photon-dominated regime with small excitonic fraction. Our task is to determine four parameters: $\zeta$, $X$, $\eta$, and $\lambda$.

Figure 1 shows the mean-field energy per excitation plotted as a function of $R_s$ for various detuning parameters $d$; however, all the curves have the same parameters, $k_c a_0 = 30$ and $\tilde{g} = 1$ (corresponds to the vacuum Rabi splitting, twice the 2D exciton Rydberg for resonant case $d = -4$, which will be accessible in distributed quantum wells [21]). We see the curves approach that of an $e$-$h$ system (dashed) and the energy saturates to the $1s$-exciton level in 2D semiconductors, $-4\varepsilon_0$, in the low-density limit, except for the strong coupling situation $|d - (-4)| \leq \mathcal{O}(g)$. This means that, at low density and large $d$, pumped energy is spent for carrier excitation, not for the generation of cavity photons; however, for the strong coupling situation with small detuning, excitations of cavity mode contribute even at the low-density limit. In the high-density region, the curves approach slightly below the photon level $d$. The energy shift from $\varepsilon/\varepsilon_0 = -4$ to $\varepsilon/\varepsilon_0 = d$ indicates the polariton condensation crossovers from excitonic to photonic ones with an increase in the excitation density. The energy saturation at high density is explained by fermionic phase-space filling of carriers and Bose statistics of the cavity photons: The number of $e$-$h$ pairs increases until the conduction electron band is filled up to the photon level, and thereafter, photonic excitations replace those of $e$-$h$ pairs to minimize the total energy. The photonic character is observed above a density ($R_s < R_s^*$) where the curves move away from the dashed curve. The crossover is directly seen in Fig. 2 where the photonic fraction in the condensate is plotted as a function of $R_s$ for the same parameter set as Fig. 1. For $R_s < R_s^*$, the photonic fraction increases sharply for large $d$ and gradually for small $d$, as the excitation density increases. Since the photonic fraction is already present in the low-density limit, the ground state can be regarded as the exciton-polariton BEC for the small $d$ case.

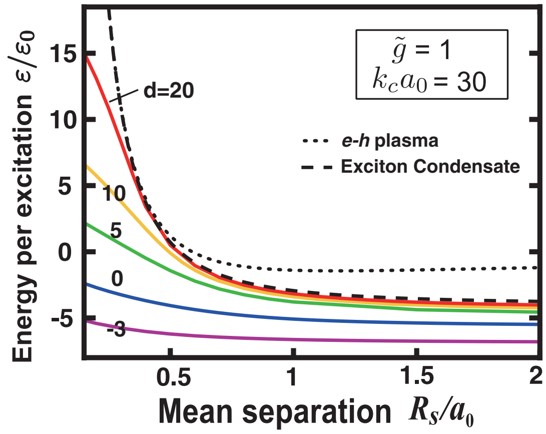


FIG. 1 (color online). Energy per excitation is plotted as a function of $R_s$ for various detuning parameters $d = 20, 10, 5, 0, -3$ with $k_c a_0 = 30$, $\tilde{g} = 1$ (solid curves). The dashed curve is obtained for $e$-$h$ systems without photons [20]. The dotted curve denotes the energy for $e$-$h$ plasma $\varepsilon/\varepsilon_0 = 2a_0^2/R_s^2 - 32a_0/(3\pi R_s)$.

In the excitonic regime where $R_s > R_s^*$, the ground state is classified into two kinds. If one excitation energy of $e$-$h$ systems (dashed curve in Fig. 1) is close to the single-exciton level $-4\varepsilon_0$, the $e$-$h$ pairs can be considered as the BEC of excitons. The low-density regime ($R_s \gtrsim 1$) is categorized as "exciton BEC." For the higher density

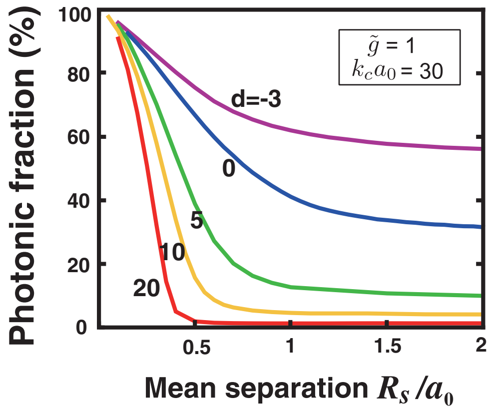


FIG. 2 (color online). Photonic fraction in the condensates plotted as a function of $R_s$ for the same parameter set as in Fig. 1.

$R_s \lesssim 1$, the binding energy becomes small as density increases (Fig. 1). Thus, the high-density regime is classified as "*e-h* BCS" where *e-h* pairs are regarded as weakly bound fermions like Cooper pairs of BCS superconductivity. In the high-density limit of the BCS regime ($R_s \lesssim 0.4$), electrons and holes are almost unbound since the curves are very close to that of *e-h* plasma (dotted curve in Fig. 1). Since $R_s^*$ varies, $d$ determines the regimes the polariton system passes through—exciton BEC and *e-h* BCS—before the ground state becomes photonlike.

Figure 3 shows the phase diagram obtained here, which contains four phases: adding to two excitonic phases, exciton BEC and *e-h* BCS, the phase diagram contains "polariton BEC" phase and "photonic BEC" phase. Although, we observe large coherent polarization and coherent photons in the latter two phases, we classified them as follows: excitations of carriers and cavity photons both make a major contribution to the condensate in polariton BEC phase, on the other hand, photonic excitations dominate over the carrier excitation in photonic BEC phase. All changes among different phases are crossovers whose boundaries are determined under certain conditions [22]. Clearly, it depends on the detuning parameter how the condensate evolves from low-density to high-density regime. For large detuning, the system experiences four types of ground states from or to exciton BEC, *e-h* BCS, polariton BEC, and photonic BEC. For small detuning, the ground state changes from polariton BEC to photonic BEC. To see the character of each phase, we plot in Fig. 4 the real space profiles of the wave function of an *e-h* pair, $P(r) = (\mathcal{N}/S)\sum_k \langle a_k^\dagger b_k \rangle \exp(ikr)$, for parameters belonging to different phases. The normalization factor $\mathcal{N}$ is chosen so that $\int dr^2 P(r)^2 = 1$. In Fig. 4(a), plots are obtained for large detuning $d = 20$ with varying $R_s$ from 3 to 0.15. The parameter values belong to the crossover regime among exciton BEC, *e-h* BCS, polariton BEC, and photonic BEC phase. Figure 4(b) is obtained for small detuning $d = 0$ with varying $R_s$ from 3 to 0.15, which corresponds to the crossover regime from polariton BEC to photonic BEC. For both plots, two similar behaviors are found: (1) At low density ($R_s = 3$), the wave function is almost the same as that of 1*s* exciton in 2D systems. (2) In photonic BEC regime at high density ($R_s = 0.15$), the wave function is sharply peaked around $r = 0$. The latter

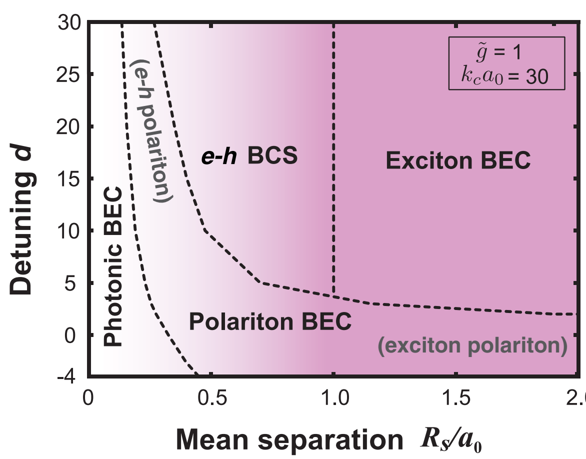


FIG. 3 (color online). Phase diagram at zero temperature is shown in $(d, R_s)$ space. Phase boundaries corresponding to a crossover are shown by the dashed lines. The region where Coulomb attraction dominates the photon-mediated interaction in the formation of *e-h* pairs is shaded (pink). Other parameters are the same as Fig. 1.

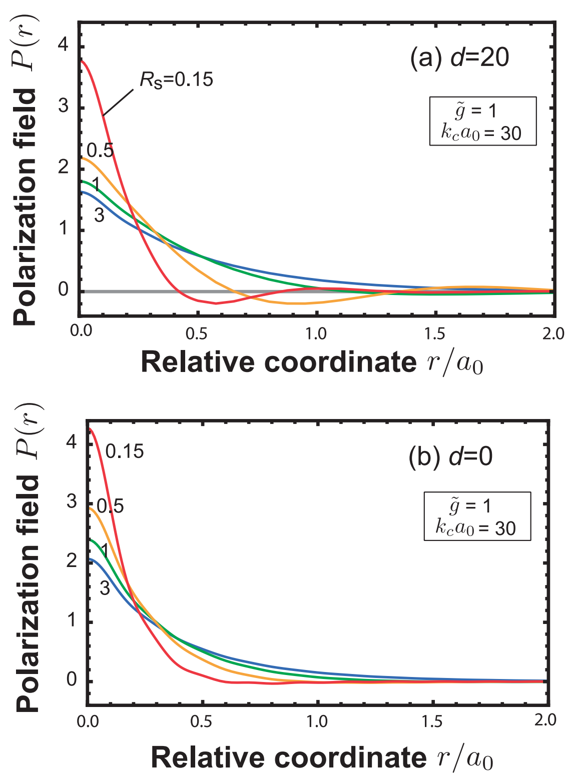


FIG. 4 (color online). Real space profiles of the *e-h* wave function $P(r)$ (normalized) for $R_s = 3, 1, 0.5, 0.15$ with different detunings: (a) $d = 20$, (b) $d = 0$. We set $\tilde{g} = 1$ and $k_c a_0 = 30$ for both.

character is due to the existence of the coherent photons at the high-density regime, i.e., as seen from the form of dipole coupling in Eq. (4), the coherent photons create $e$-$h$ pair at the same position $[P(r = 0)]$. In other words, the coherent photon field produces an attractive delta potential $\propto \delta(r)$ for an $e$-$h$ pair. The two behaviors show that as the polariton BEC changes from excitonic to photonic, the binding force between an $e$-$h$ pair changes from Coulomb attraction to a short-range attraction mediated by photon. The Coulomb dominated regime is shaded in Fig. 3. Accordingly, polaritons are composite bosons of photons and excitons (free $e$-$h$ pairs) in the shaded (unshaded) area of polariton BEC phase. The difference between highly and slightly detuned cases is found in the tails of the wave function. For the highly detuned case, oscillation behavior is found at high density ($R_s = 0.15, 0.5$), which is not seen in the slightly detuned case. The oscillation is due to the formation of the Fermi surface in the carrier distribution function, and the period is given by the Fermi wavelength.

Finally, we comment on the strong binding of an $e$-$h$ pair, which is expected for photonic regime of the large cutoff case. As noted above, the $e$-$h$ pairing is due to photon-mediated short-range attraction in the photonic regime [23]. The short-range attraction causes the strongly bound pairs with small radius which is determined by the inverse of the cutoff momentum $k_c$. Since the radius will be of the same order as the lattice constant $\sim 1/k_c$, an $e$-$h$ pair should be recognized as a Frenkel exciton, and hence, the description is beyond the capability of our model which employs the effective mass approximation. This indicates the need for other models to treat excitons with small radius such as the Dicke model [13,14]. As well, in the photonic regime, the main contribution to $P(r = 0)$ comes from $e$-$h$ pairs $\langle a_k^\dagger b_k \rangle \propto k^{-2}$ for $k \gg 1/a_0$, resulting in the cutoff dependencies $P(0) \propto \log(\kappa_c)$ in 2D systems and $\propto \kappa_c$ in 3D systems. This indicates the photon-mediated attraction is stronger in 3D than in 2D systems. Moreover, in experiments [24], normal lasing (kinetic regime) is observed at high density before the system enters the photonic BEC regime for certain reasons: carrier heating [24] or shortening of the lifetime of polaritons in the photonic regime [11]. However, if excitation with quantum degeneracy were achieved up to sufficiently high density (possible in the future), the photonic BEC will be observed and a clear difference from lasing will be found in the optical spectrum. We found in our calculation that the electron distribution function $f_e(k) = v_k^2$ develops the plateau at $f_e \approx 0.5$ spread over $k$ space [13,25]. No such feature is expected in the normal lasing, and instead, a dip in $f_e$ at a momentum corresponding to the laser frequency will be found (spectral hole burning [26]). The characteristic emission spectrum in the photonic BEC is also discussed in Ref. [25], which refers to the possible observation of Mollow's triplet.

In summary, the mean-field ground states of microcavity polaritons are determined by a variational approach [20]. The ground state changes from excitonic to photonic as a function of the density and the detuning. In the photonic regime, $e$-$h$ pairs are shown to be bound in a small radius by photon-mediated delta attraction.

We thank P. Littlewood, Y. Yamamoto, K. Asano, T. Ohashi, and K. Watanabe for fruitful discussions. We acknowledge support by KAKENHI (20104008) and Funding Program for World-Leading Innovative R&D on Science and Technology.

*kamide@acty.phys.sci.osaka-u.ac.jp

[1] J. Kasprzak *et al.*, Nature (London) **443**, 409 (2006).
[2] R. Balili *et al.*, Science **316**, 1007 (2007).
[3] J. J. Baumberg *et al.*, Phys. Rev. Lett. **101**, 136409 (2008).
[4] S. A. Moskalenko and D. W. Snoke, *Bose-Einstein Condensation of Excitons and Biexcitons* (Cambridge University Press, Cambridge, England, 2000).
[5] M. H. Szymańska *et al.*, Phys. Rev. Lett. **96**, 230602 (2006).
[6] M. Wouters *et al.*, Phys. Rev. Lett. **99**, 140402 (2007).
[7] L. Pitaevskii and S. Stringari, *Bose-Einstein Condensation* (Oxford Science, Oxford, 2003).
[8] S. Utsunomiya *et al.*, Nature Phys. **4**, 700 (2008).
[9] K. G. Lagoudakis *et al.*, Nature Phys. **4**, 706 (2008).
[10] A. Amo *et al.*, Nature Phys. **5**, 805 (2009).
[11] J. Kasprzak *et al.*, Phys. Rev. Lett. **101**, 146404 (2008).
[12] D. Bajoni *et al.*, Phys. Rev. Lett. **100**, 047401 (2008).
[13] P. R. Eastham *et al.*, Phys. Rev. B **64**, 235101 (2001).
[14] J. Keeling *et al.*, Phys. Rev. B **72**, 115320 (2005).
[15] F. M. Marchetti *et al.*, Phys. Rev. B **70**, 155327 (2004).
[16] F. M. Marchetti *et al.*, Solid State Commun. **134**, 111 (2005).
[17] Y. Yamamoto and A. Imamoglu, *Mesoscopic Quantum Optics* (John Wiley & Sons, New York, 1999).
[18] C. A. Regal *et al.*, Phys. Rev. Lett. **92**, 040403 (2004).
[19] M. Holland *et al.*, Phys. Rev. Lett. **87**, 120406 (2001).
[20] C. Comte and P. Nozieres, J. Phys. (Paris) **43**, 1069 (1982); P. Nozieres and C. Comte, *ibid.* **43**, 1083 (1982).
[21] J. Bloch *et al.*, Appl. Phys. Lett. **73**, 1694 (1998).
[22] $R_s^*$ is defined by the density above which the photonic fraction becomes larger than 20%. At low density ($R_s > R_s^*$), the boundary between exciton BEC and $e$-$h$ BCS is given by $R_s = 1$. We defined "polariton BEC" as the density region where the photonic fraction is larger than 20% and less than 80%. If the fraction is larger than 80%, the BEC is regarded to be photonlike, and the corresponding regime is defined as "photonic BEC."
[23] K. Kamide and T. Ogawa, J. Phys. Conf. Ser. **210**, 012021 (2010).
[24] H. Deng *et al.*, Proc. Natl. Acad. Sci. U.S.A. **100**, 15 318 (2003).
[25] T. Byrnes *et al.*, arXiv:1005.3141.
[26] H. Haken, *Light: Laser Light Dynamics* (North-Holland, Amsterdam, 1986).